

## Accelerated Corrosion Test in Mortars of Plastic Consistency with Replacement of Rice Husk Ash and Nano-SiO<sub>2</sub>

M. J. Pellegrini Cervantes<sup>1</sup>, C.P. Barrios Durstewitz<sup>1,\*</sup>, R. E. Núñez Jaquez<sup>1</sup>, F. Almeraya Calderón<sup>2</sup>, M. Rodríguez Rodríguez<sup>1</sup>, G. Fajardo-San-Miguel<sup>4</sup>, A. Martínez-Villafañe<sup>5</sup>

<sup>1</sup>Universidad Autónoma de Sinaloa Facultad de Ingeniería Mochis, Fuente de Poseidón y Prol. Ángel Flores S/N, Los Mochis, Sinaloa, México.

<sup>2</sup>Universidad Autónoma de Nuevo León. FIME - Centro de Innovación e Investigación en Ingeniería Aeronáutica. Av. Universidad s/n. Ciudad Universitaria. San Nicolás de los Garza, N.L., México.

<sup>3</sup>Universidad Veracruzana, Facultad de Ingeniería Civil-Xalapa, Circuito Gonzalo Aguirre Beltrán s/n, Zona Universitaria 91000, Xalapa, Veracruz, México.

<sup>4</sup>Facultad de Ingeniería Civil, Universidad Autónoma de Nuevo León

Av. Universidad S/N, C.U. San Nicolás de los Garza, N.L. C.P. 66450, México.

<sup>5</sup>Departamento de Integridad y Diseño de Materiales Compuestos. Centro de Investigación en Materiales Avanzados. S.C. CIMAV. Miguel de Cervantes No. 120, Complejo Industrial Chihuahua, C.P 31109, Chihuahua, Chihuahua, México.

\*E-mail: [durstewitz@uas.edu.mx](mailto:durstewitz@uas.edu.mx)

Received: 31 January 2015 / Accepted: 3 March 2015 / Published: 26 August 2015

---

Cement replacement by ash in mortars has ecological and microstructural advantages. Meanwhile, nanoparticles (NP) replacements improve the performance of properties at nanometer scale. Researchers have incorporated in mortars nano Silica Oxide (nSO) and rice husk ash (RHA) through studies of physical and mechanical properties. However, the study of the synergy of their simultaneous use is scarce mainly regarding the resistance to corrosion. This paper evaluated the performance of properties of plastic consistency mortars with replacement of ordinary Portland Cement (OPC) by 20% RHA and 1.0% nSO, by assaying porosity, compressive strength and resistance to corrosion by impressed voltage. The simultaneous replacement of RHA+nSO resulted in higher performance, with decreases in superficial absorption up to 60.0%, decreases in porosity up to 3.9% and increased compressive strength and corrosion of 7.1% and 37.6%, respectively. Simultaneous use of RHA+nSO of plastic consistency mortars presents advantages in the improvement of electrochemical, physical and mechanical properties, due to the synergistic effect of the combination of ash and nanoparticles.

---

**Keywords:** superficial absorption, nanometric mortar, accelerated corrosion, nanoparticles.

## 1. INTRODUCTION

The durability of reinforced mortar is demerited with the corrosion of the reinforcement, with determining factors such as the structure and pore distribution, effective porosity and mechanical strength [1]. Researchers have replaced the OPC with different types of ashes with the purpose of providing durability to mortars, with satisfactory results. The replacement of OPC by ashes as: RHA [2,3], fly ash (FA), blast furnace ash, ash bagasse, among others [4-9], decreases the effects of corrosion of the reinforcement produced in harsh environments and improves mechanical, structural, physical, chemical and electrochemical properties [10-12]. In the particular case of RHA, it is a waste product of power generation in industrial plants that can be used as a replacement for OPC. The replacement of OPC by RHA improves the properties of the cement mass of mortar and also contributes to the environmental aspect by reducing by its use the need of cement production, which generates high levels of pollution [13]. Other OPC replacements with which increases were obtained in the performance of physical, chemical and mechanical properties are the NP [14].

NP have also been used as replacement for OPC in mortars and concrete with improvement in their properties at the nanoscale, NP such as nSO [15- 17] Iron and Titanium oxide, among others [17]. In addition, the simultaneous use of NP and ash produces a synergistic effect that increases the performance of the properties of mortars at early ages and increases its durability in harsh environments [18- 21]. However, investigations where it is addressed the study of the simultaneous use of ash and NP as a replacement of cement are scarce and focused only to certain kind of materials, few with scientific reports that address the issue of durability and corrosion in reinforced mortars with replacements of OPC by nSO and RHA in simultaneous use [18-22]. The replacement of OPC by RHA and nSO in simultaneous use should favor the microstructure of cement mass and obtain nanometric mortars with a more compact matrix, higher mechanical performance and resistance to corrosion.

The purpose of this work was to study the performance of nanometric mortars of plastic consistency through studies of total porosity, effective porosity, mechanical strength and resistance to corrosion in a reinforced mortar by replacing OPC by RHA and nSO individually and simultaneously, with replacement of 20% RHA and 1% nSO of the total cementitious weight.

## 2. EXPERIMENTAL PROCEDURE

### 2.1 Materials

For the manufacture of the specimens, fine aggregate, OPC, RHA, nSO, distilled water and superplasticizer (SP) were used. The fine aggregate was silica sand river, graded according to ASTM C 33-03 [25], fineness modulus of 2.61, mass density 2660 kg/m<sup>3</sup> and 3.7% absorption. The physical properties of cementitious materials are shown in

Table 1. The SP was a high rank water-reducing additive of short delay without chlorides type F and type I, according to ASTM C 494/C 494M – 99a [26] and C1017 / C1017M - 07 [27]. The OPC was supplied by local cement company, while the RHA was obtained from industrial wastes of Odisha, India, ground in Los Angeles apparatus for 2 hr. and sieved in mesh No. 325 (opening 45 μm). The

nSO was commercially obtained without any additional treatment for its use. The chemical properties of OPC, RHA and nSO, according to chemical analysis of Gravimetry (G) and Stoichiometry (S) are shown in Table 2 and Scanning Electron Microscopy (SEM) of cementitious in Figure 1. Furthermore, the Rx dispersion analysis of nSO is shown in Figure 2.

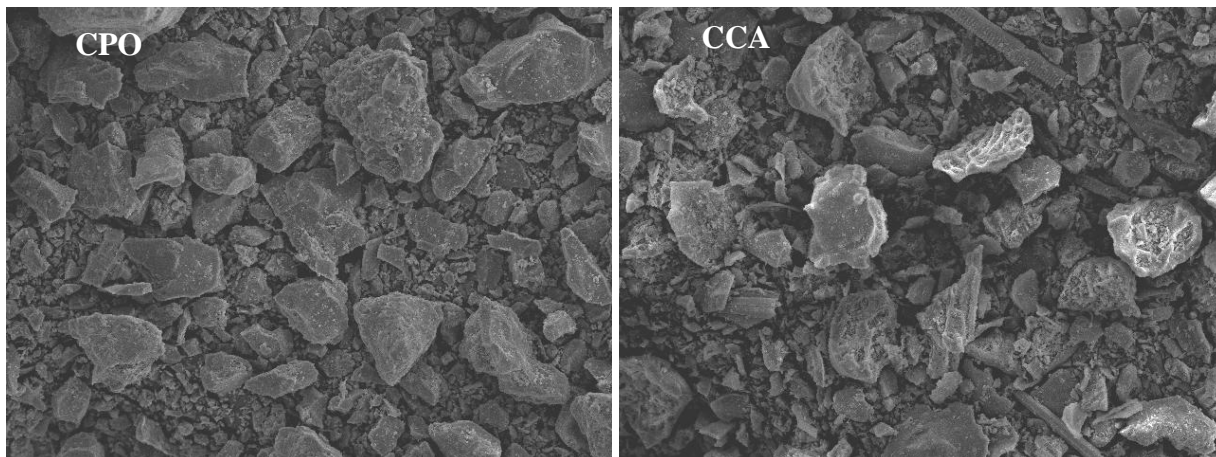


Figure 1. Ordinary Portland Cement and rice Husk Ash SEM (x500).

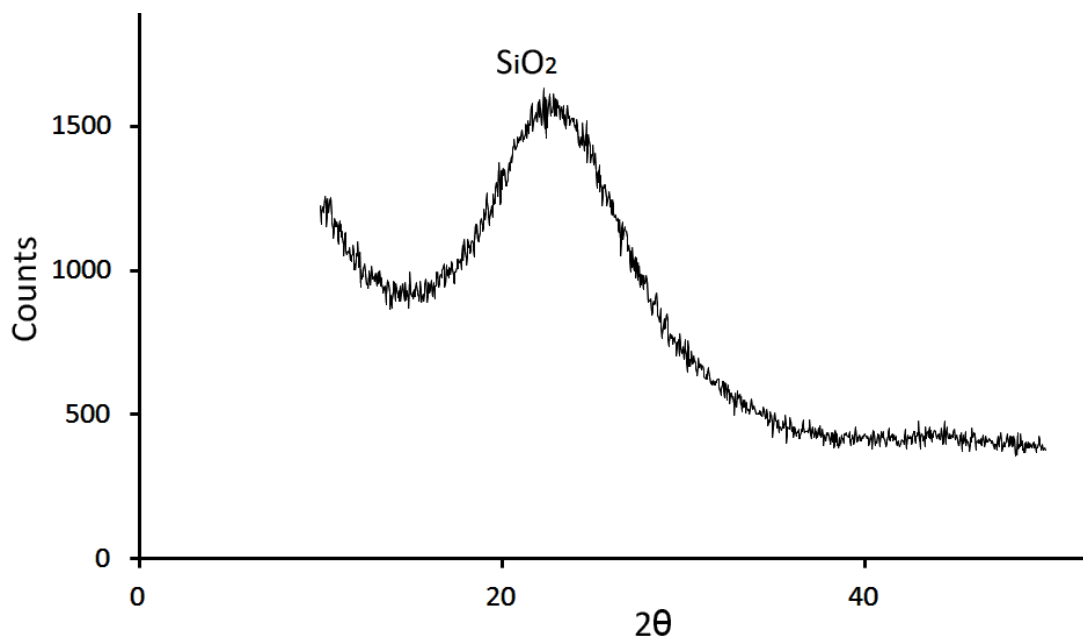


Figure 2. nSO Rx Dispersion.

Table 1. Physical properties of cementitious materials.

Property	OPC	RHA	nSO
Mass density (kg/m <sup>3</sup> )	3071	2251	-
Superficial area (m <sup>2</sup> /g)	20.23	23.82	777.7
Average particle size (Φm)	27.61	29.88	0.015

**Table 2.** Chemical components of materials.

Oxide	OPC	RHA	nSO	Analysis method
SiO <sub>2</sub>	20.046	84.375	71.451	G
SO <sub>3</sub>	2.589	0.080	-	S
CaO	2.605	0.702	-	S
Fe <sub>2</sub> O <sub>3</sub>	1.976	0.309	-	S
MgO	0.762	0.276	-	S
K <sub>2</sub> O	0.317	1.242	-	S
Al <sub>2</sub> O <sub>3</sub>	0.294	0.235	N.D.*	S
TiO <sub>2</sub>	0.228	0.018	-	S
P <sub>2</sub> O <sub>5</sub>	0.123	0.566	-	S
MnO	0.048	0.103	-	S
Na <sub>2</sub> O	0.007	0.057	0.003	S

\*N.D. Not Detected

## 2.2 Preparation of mixture and specimens.

In mortar mixtures a water/cementitious ratio (W/C) of 0.55 and sand/cementitious ratio of 2.75 were used, incorporating an SP in order to obtain mortar mixtures with similar flow of  $110 \pm 5\%$ . The dosage of the cementitious mortar mixtures is shown in **Error! Reference source not found.**

**Table 3.** Dosing in cementitious mortar mixtures (%).

Mixture	OPC	RHA	nSO
M100-0-0	100.0	0.0	0.0
M80-20-0	80.0	20.0	0.0
M99-0-1	99.0	0.0	1.0
M79-20-1	79.0	20.0	1.0

The mixing procedure was similar to ASTM C 305-12 [28] with some variants according to [20-22] :

- 1) If the mixture contained RHA, it was dry blended with OPC until achieving a uniform consistency.
- 2) If the mixture contained nSO, 95% of the total water of the mixture was added; it was then subjected to ultrasonic dispersion for 10 min.
- 3) Cementitious material was added to 95% of water; it was then mixed for 30 sec. at slow speed.
- 4) The mixer was stopped and changed to medium speed; it was then mixed for 30 sec. while the sand was slowly added during that period.
- 5) After mixing for 30 sec. at medium speed, the SP + 5% of water were slowly added in the first 10 sec.

- 6) After stopping the mixer, it remained in rest for 90 sec. In the first 15 sec. the walls of the container were quickly scraped and the mixture was covered for the remaining time.
- 7) Finally, it was mixed for 90 sec. at medium speed.

The mixture flow was verified according to ASTM C 1437-99 [29], then the mixture was poured into P.V.C. molds and covered with plastic for 24 hr. until hardened.

## 2.2 Total porosity and compressive strength.

The compressive strength was performed according to ASTM C 109/C 109M-05 [30] in cubic specimens of 2.5 cm side. After test, the residues of the specimens were immersed in methanol for SEM analysis.

The porosity of the hardened mortar was determined according to equation (1). The method used was in vacuum saturated condition, successfully accepted method by several authors for the calculation of porosity in cementitious materials [31, 32].

$$P (\%) = 100 * \frac{W_a - W_d}{W_a - W_w} \quad (1)$$

Where:

P= Total Porosity (g).

$W_a$ = Specimen weight in saturated conditions (g). The saturated condition is achieved by 1 hr. vacuum in air, 3 hr. of submerged vacuum in deaerated water and 20 hr. of submerged at ambient pressure.

$W_d$ = Dry specimen weight after 24 hr. of drying in an oven at  $100 \pm 5$  ° C (g).

$W_w$ = Specimen weight in saturated conditions submerged in water (g).

Both tests were performed at 30 and 90 days of curing in distilled water, 100% relative humidity and temperature of  $23 \pm 2$  °C. The results reported are the average of three tests.

## 2.3 Accelerated corrosion test with impressed voltage.

ACTIV provides an indirect comparison parameter for estimating the corrosion resistance of cementitious materials [32]. The specimens were 4.0x4.0x16.0 cm, reinforced with steel rods 0.95 cm in diameter and 16.0 cm long as shown in Figure 3. Steel was protected at the air-mortar interface, coating of 1.5 cm and steel surface exposed to the environment of 37.3 cm<sup>2</sup>.

After 90 days of curing, the specimens were subjected to ACTIV under arrangement as show in Figure 4 , they were immersed in aqueous solution at 5% NaCl by applying constant voltage  $12 \pm 0.1$  V at a temperature of  $25 \pm 2$  °C.

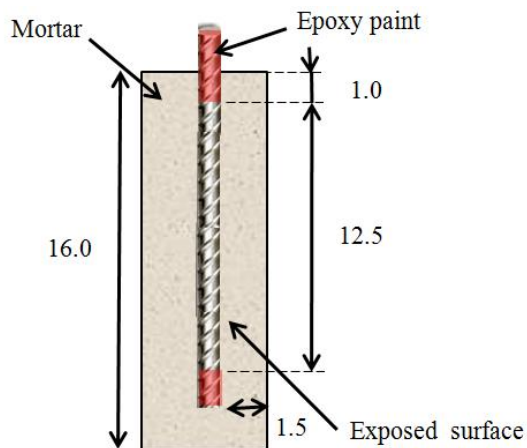


**Figure 3.** Steel reinforcement and reinforced mortar specimen.

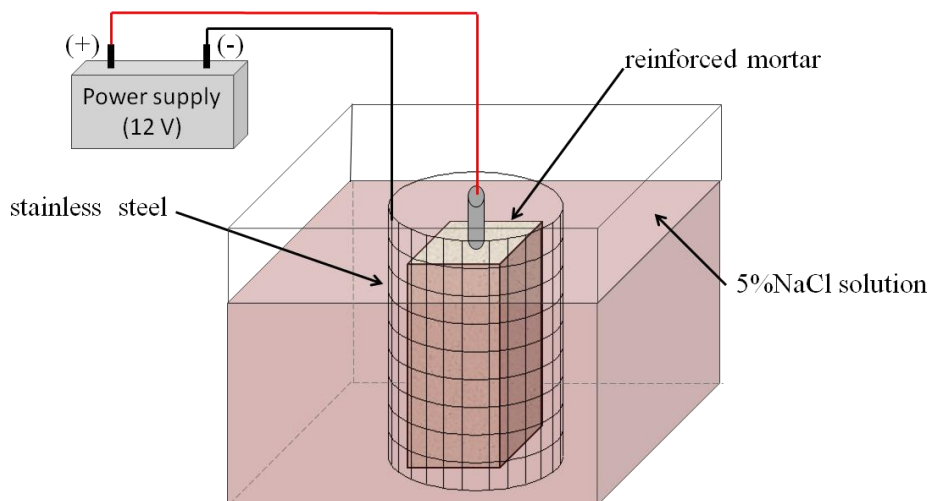


**Figure 4.** Experimental arrangement ACTIV.

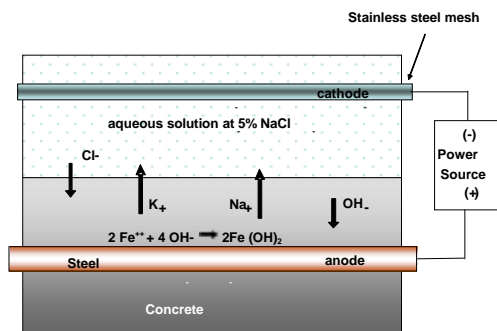


**Figure 5.** ion movement during ACTIV.

There is a natural process of diffusion of chloride ions before ACTIV, after ACTIV with the application of the impressed current the reinforcing steel remains totally unprotected by the charge supplied to it, where the process of the migration of the chloride ions occurs towards the anode surface, the ionic movement during ACTIV is shown in figure 5.

Before ACTIV the specimen exhibits no cracks in the mortar mass, after ACTIV is applied the corrosion products generated in the steel surface begin to occur and end with the cracking of the mortar mass, as shown in figure 6. The condition of the prism was monitored continuously until cracking of the specimen, recording the time of initiation of the first crack (TIFC). The results reported are the average of three tests.

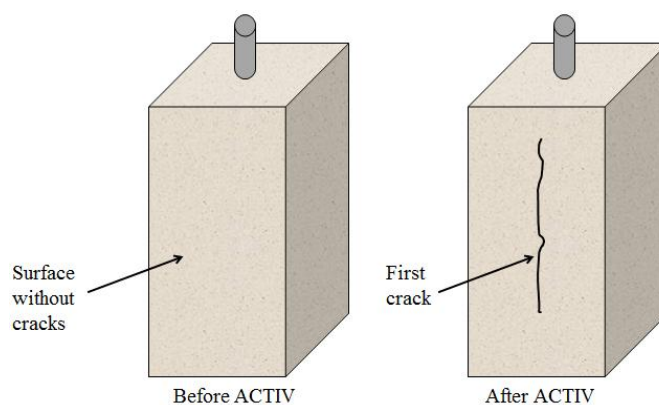


**Figure 6.** Initiation of the first crack.

### 2.3 Absorption test by pipette.

In Absorption Test by Pipette (ATP), the mortar specimens used were with A/Cm of 0.50 for ages of 28 and 90 days, performing assay according to RILEM II.4 recommendations (RILEM, 1980). The test specimens were dried in oven at  $60 \pm 5$  °C until a constant dry mass, setting the pipette with silicone on central zone of one of the sides of the test specimen. Next, distilled water was added into the pipette up to a liquid column of 13.25 cm. above the surface of mortar, being of 2.50 cm. the diameter in the contact zone with mortar and 0.84 cm in the main column. ATP was performed at  $25 \pm 2$  °C. ambient temperature. Finally, the absorbed water volume was measured versus time every hour for 24.0 h., graphing the results obtained with absorption in  $\text{cm}^3$  in vertical axis against time in hours in horizontal axis. The results reported are the average of three assays.

## 3. RESULTS AND DISCUSSION

### 3.1 Materials

The use of RHA and nSO as replacement OPC provides higher performance to the properties of mortar and concrete, creating products that serve to fill in the gaps in the matrix [3, 15, 20-22].

According to SEM shown in Figure 1, the particles that make up the RHA are irregular and with sharp edges, size from 1.7 to 45.4  $\mu\text{m}$ , they are also irregular in OPC but having softer edges with sizes from 1.3 to 63.0  $\mu\text{m}$ . The OPC has finer particles than the RHA. The RHA is a natural ash calcined Type N according to ASTM C618-99 [30], with  $\text{SiO}_2 + \text{AlO}_3 + \text{F}_2\text{O}_3 > 70\%$  y  $\text{SO}_3 < 4.0\%$ . The nSO has a content of  $\text{SiO}_2$  of 71.45%, higher OPC and less than RHA. The particle size distribution of the cementitious, their physical and chemical properties define the microstructure of the hardened mortar.

### 3.2 Mortar Mixtures and morphology of hardened mortar

Calcined ashes have an hygroscopic nature and high superficial area, its use brings mixtures requiring more water or SP for an equivalent desired flow [34, 35, 20-22]. In mixtures made in this study, the replacement of OPC by RHA and nSO in simultaneous use increased the amount of SP, with 0.9, 2.2, 1.5 and 2.8% for M100-0-0, M80-20-0, M99-0-1 and M79-20-1 respectively. The increase in surface area due to nSO and RHA replacements in conjunction with the hygroscopic nature of RHA contributed to the increase of SP. The properties of the mixture in the fresh state and the curing conditions help to determine the microstructure of the hardened mortar.

The uniform dispersion of nSO has an important role in improving the microstructure of the cement matrix [36]. Hardened Mortars microstructure is shown in Figure 7. In general, the replacement of OPC by RHA+nSO in simultaneous use produced morphologies of the cement matrix more compact than in the case of the absence of replacements or in the individual use of nSO and RHA, which is attributed to the generation of hydration products that fill the pores network of the matrix. The microstructure of the cement matrix defines to a great extent the properties of porosity, permeability and mechanical resistance of the hardened mortar.

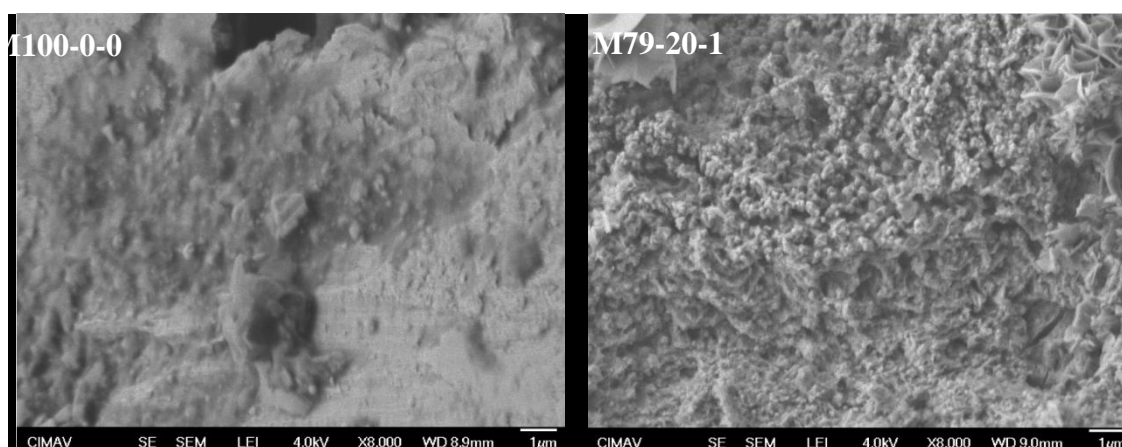


**Figure 7.** SEM hardened mortar aged 90 days.

### 3.2 Total porosity and compressive strength.

The replacement of OPC by RHA increases the performance of the total porosity of mortar decreasing at greater amount of RHA [20-22, 35]. On manufactured hardened mortars, total porosities

for ages 30 and 90 days are shown in Figure 8. For the use as individual replacement of RHA, porosity increased 5.1 and 3.9% for 30 and 90 days respectively, which is attributed to the used amount of SP that has a demerit effect in this property. However, the replacement of nSO either individually or simultaneously, favored the decrease in porosity, presenting at 30 days the lowest porosity in M99-0-1. As at 90 days of age, the simultaneous replacement of RHA+nSO resulted in higher performance even lower than M99-0-1, with less porosity in M79-20-1 and decrease of 3.9% with respect to M100-0-0. Therefore, replacement of OPC by nSO increases the porosity performance both in individual and in simultaneous use and manages to counteract the increase in porosity caused by the use of SP in the mix. Several investigations [2, 3, 14, 15] demonstrate the favorable effect of replacement of OPC by RHA or nSO respect to physical properties, besides bringing benefits in mechanical properties.

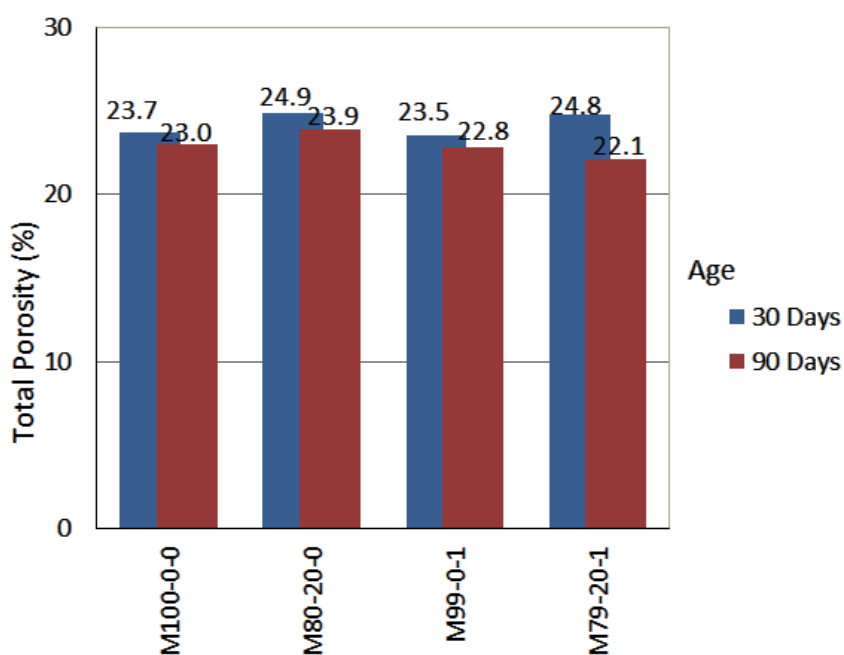


Figure 8. Total porosity of hardened mortars

The compressive strength of hardened mortar increases its performance with replacements of OPC by RHA [18]. The results of simple compression resistance in manufactured hardened mortars are shown in Figure 9. The performance of the porosity increased with the presence of nSO at age 30 and 90 days, with maximum performance in simultaneous use of RHA and nSO for both ages and increases of 7.2 and 7.1% at 30 and 90 days, respectively. Based on the results, performance increases with the replacement of RHA, surpassed for nSO replacements and with higher compressive strengths with the simultaneous use of RHA+nSO. As well as the mechanical properties are important in the performance of cementitious materials, so is its resistance to corrosion.

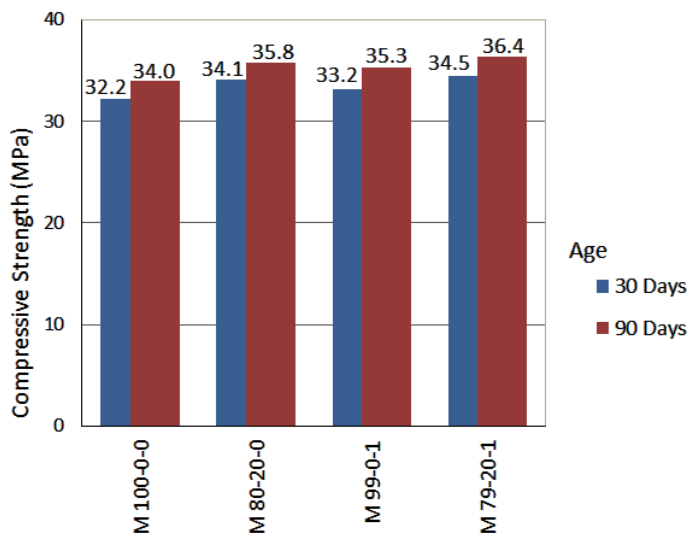


Figure 9. Compressive strength of hardened mortar

3.3 Accelerated corrosion test with impressed voltage.

The replacement of OPC by 20% of RHA in mortar of plastic consistency increases the resistance to corrosion up to 83.0% [32]. For manufactured reinforced mortars, TIFC results by ACTIV are shown in Figure 10 and test specimens after ACTIV in Figure 11. In every mix prepared, at replacing OPC by RHA or nSO individually or simultaneously, TIFC increased compared to reference. For individual replacement of OPC by RHA the increase was of 32.3% in individual use of nSO of 30.1% and in simultaneous use of RHA+NOS was 37.6%. The order in the increasing of the performance of the ACTIV corresponds to that shown in compressive strength, which is congruent since the mechanical strength is a determinant factor for the presence of the first crack. Based on the results, the replacement of OPC by RHA+nSO in simultaneous use increases the performance of resistance to corrosion at higher levels than the individual use of the replacements.

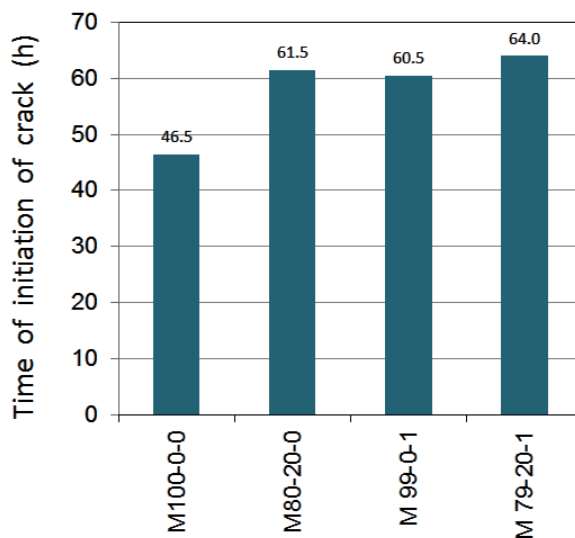


Figure 10. TIFC in accelerated corrosion test with impressed voltage.



**Figure 11.** Reinforcement steel after ACTIV.

Impressed voltage on the surface of the reinforcing steel increases the velocity of movement of the chloride ions in the cement mortar mass. With the advent of the chloride ion to the surface of the steel corrosion products are generated and they induce tension stresses into the mortar mass, by exceeding the resistance to tension of the cementitious material cracks begin to show, as shown in Figure 11. The potential difference induced by impressed voltage causes that the reinforcement rod becomes an anode with chemical attack from chloride ions, being the pores of the cement matrix the ionic transport route. Mortars with RHA+nSO show greater resistance to corrosion because their TIFC is greater, being congruent because it is the one with the lower porosity and greater compressive strength.

3.3 Absorption test by pipette.

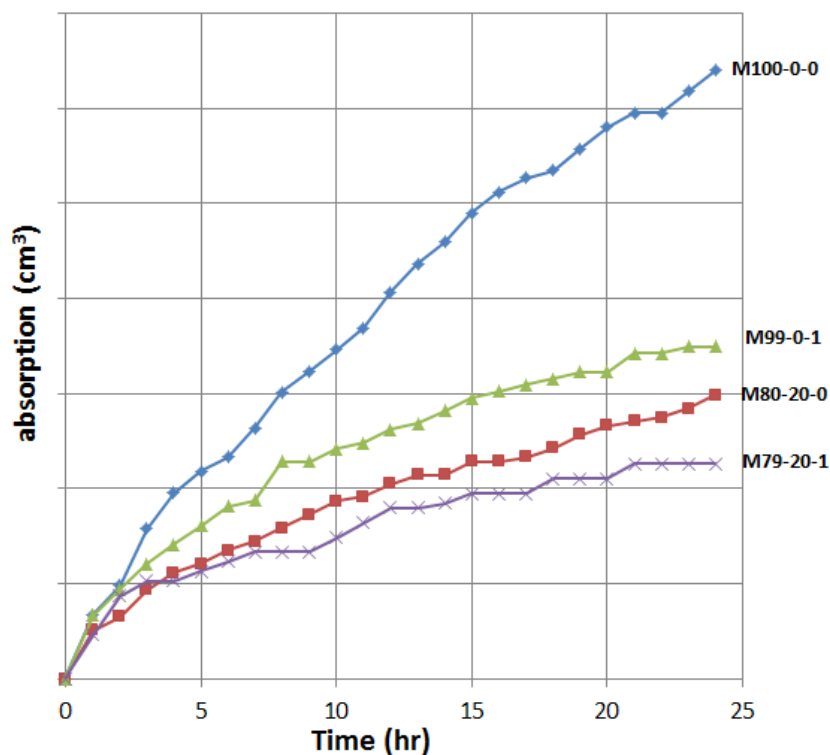


**Figure 12.** Pipette absorption in mortars, A/cm=0.55 to 30 days age.

The results of the absorption test can be used to evaluate the vulnerability of materials to deterioration caused by contact with water (RILEM, 1980). In mortars made, surface absorption of different mixtures is shown in Figure 12, the cement replacement by RHA reduces superficial absorption significantly up to 53%, while by simultaneously replacing RHA+NOS the decrease in the superficial absorption is of higher performance than with the single use of RHA as of nSO with decreases of up to 65%. Therefore, the simultaneous use of RHA+NOS as a replacement for cement results in higher performance than in the single use of RHA or nSO, due to the hydration products generated by the use of nSO.

#### 4. CONCLUSIONS

The results of this study show that:

Producing mortar with plastic consistency with the replacement of OPC by RHA and nSO is possible with the use of SP and ultrasonic dispersion of nSO. The use of SP affects the performance of the synergy by simultaneous use of RHA and nSO in mortars, owing to its high percentage of use for the production of mixtures.

The porosity in mortars of plastic consistency has higher performance with the individual use of nSO at 30 days of age, decreasing to 0.8% of reference. The surface absorption increased its performance with the simultaneous use of RHA+NOS, decreasing 65% of reference. However, it has a maximum yield of 20% RHA in simultaneous use and 1% nSO at 90 days, decreasing to 3.9% of reference. The compressive strength has a maximum performance in simultaneous use of 20% RHA + 1% nSO at 30 and 90 days, increasing 7.14 and 7.06% of reference, respectively. The resistance to corrosion has a better performance in simultaneous use of 10% RHA + 1% nSO at 90 days, increasing the time of initiation of the first crack to 37.6% of reference.

Based on the results, the replacement of OPC by RHA and nSO in simultaneous use in mortars of plastic consistency is advantageous in the performance of physical, mechanical and corrosion resistance properties, due to the synergy of RHA and nSO for replacements of 20% RHA and 1% NOS.

#### ACKNOWLEDGEMENTS

The authors express their gratitude to the Universidad Autónoma de Sinaloa (UAS) for the financial support and to Grupo Cementos Chihuahua (GCC) and SIKA Corp for the support material supply. The first author would like to thank Centro de Investigación en Materiales Avanzados (CIMAV) and Universidad Autónoma de Nuevo Leon (UANL) for its support in the accomplishment of the present work.

#### References

1. R. Kumar and B. Bhattacharjee, *Cement and Concrete Research*, 33 (2003) 417-424.
2. B. Chatveeraa and P. Lertwattanaruk, *Journal of Environmental Management*, 92 (2011) 59-66.

3. A. A. Ramezaniyanpour, M. Mahdi khani and G. Ahmadibeni, *International Journal of Civil Engineering*, 7 (2009) 83-91.
4. M. Sahmaran and V.C. Li, *Cement and Concrete Research*, 39 (2009) 1033–1043.
5. M. Bohác and M. Gregerova, *Materials Characterization*, 60 (2009) 729–734.
6. K. Ganesan and K. Rajagopal, *Anti-Corrosion Methods and Materials*, 54 (2007) 230-236.
7. S. Rukzon and P. Chindapasirt, *Indoor Built Environment*, 18 (2009) 313-318.
8. C. H. K. Lam, A. W. M. Ip, J. P. Barford and G. McKay, *Sustainability*, 2 (2010) 1943-1968.
9. U. I Hernández Toledo, R. Alavéz Ramírez and P. Montes García, *Naturaleza y Desarrollo*, 7 (2009) 34–45.
10. V. Saraswathy and H.W. Song, *Construction and Building Materials*, 21 (2007) 1779–1784.
11. B. H. Abu Bakar, R. Putrajaya and H. Abdulaziz, *Concrete Research Letters*, 1 (2010) 6–13.
12. Tae-Hyun Ha, S. Muralidharan, J.H. Bae, Y.C. Ha, H.G. Lee, K.W. Park and D.K. Kim, *Building and Environment*, 42 (2007) 78–85.
13. P.K. Mehta. *In: Advances in concrete technology*, 2nd ed.(1994) 419–44..
14. F. Pacheco Torgal and S. Jalali, *Construction and Building Materials*, 25 (2011) 582-590.
15. A. Nazari and S. Riahi, *Composites: Part B*, 42 (2011) 570-578.
16. A. Naji Givi, S. A. Rashid, F. N. A. Aziz and M. A. Mohd Salleh, *Composites: Part B*, 42 (2011) 562-569.
17. A. Naji Givi, S. A. Rashid, F. N. A. Aziz and M. A. Mohd Salleh, *Composites: Part B*, 41 (2010) 673-677.
18. T. Ji, *Cement and Concrete Research*, 35 (2005) 1943–1947.
19. Y. Qing, Z. Zenan, K. Deyu and C. Rongshen, *Construction and Building Materials*, 21 (2007) 539–545.
20. M.J. Pellegrini Cervantes, F. Almeraya Calderon, A. Borunda Terrazas, R.G. Bautista Margulis, J.G. Chacón Nava, G. Fajardo San Miguel, J.L. Almaral Sanchez, C.P. Barrios Durstewitz and A. Martinez Villafañe, *International Journal of Electrochemical Science*, 8 (2013) 10697 - 10710.
21. M.J. Pellegrini Cervantes, F. Almeraya Calderon, F.J. Baldenebro Lopez, R.E. Nuñez Jaquez, G. Fajardo San Miguel, J.G. Chacón Nava, C.P. Barrios Durstewitz, A. Martinez Villafañe, *IOSR Journal of Engineering (IOSRJEN)*, 3 (2013) 24-30.
22. M.J. Pellegrini-Cervantes, F. Almeraya-Calderon, A. Borunda-Terrazas, R.G. Bautista-Margulis J.G. Chacón-Nava, G. Fajardo-San-Miguel, J.L. Almaral-Sanchez, C.P. Barrios-Durstewitz, A. Martinez-Villafañe, *International Journal of Electrochemical Science*, 10 (2015) 332 - 346.
23. D.F. Lin, K.L. Lin, W.C. Chang, H.L. Luo and M.Q. Cai, *Waste Management*, 28 (2008) 1081–1087.
24. K.L. Lin, W.C. Chang, D.F. Lin, H.L. Luo and M.C. Tsai, *Journal of Environmental Management*, 88 (2008) 708–714.
25. ASTM C33-03, Standard Specification for Concrete Aggregates, Book of standards, vol. 04.02 (2003).
26. ASTM C 494/C 494M – 05a, Standard Specification for Chemical Admixtures for Concrete, Book of standards, vol. 04.02 (2005).
27. ASTM C1017 / C1017M - 07, Standard Specification for Chemical Admixtures for Use in Producing Flowing Concrete, vol. 04.02 (2007).
28. ASTM C 305-12, Standard Practice for Mechanical Mixing of Hydraulic Cement Pastes and Mortars of Plastic Consistency, vol. 04.01 (2012).
29. ASTM C 1437-99, Standard Test Method for Flow of Hydraulic Cement Mortar, vol. 04.01 (1999).
30. ASTM C 109/C 109M – 05, Standard Test Method for Compressive Strength of Hydraulic Cement Mortars (Using 2-in. or [50-mm] Cube Specimens), vol. 04.01 (2005).
31. S. Rukzon, P. Chindapasirt and R. Mahachai, *International Journal of Minerals, Metallurgy and Materials*, 16 (2009) 242-247.
32. P. Chindapasirt and S. Rukzon, *Construction and Building Materials*, 22 (2008) 1601-1606.

33. ASTM C 618 – 99, Standard Specification for Coal Fly Ash and Raw or Calcined Natural Pozzolan for Use as a Mineral Admixture in Concrete, vol. 04.02 (1999).
34. P.K. Metha. In: Proceeding of work shop on rice husk ash cement, (1979) 113–22.
35. P. Chindaprasirt and S. Rukzon, *Construction and Building Materials*, 22 (2008) 1601-1606.
36. H. Li, H. G. Xiao, J. Yuan and J. Ou, *Composites Part B: Engineering*, 35 (2004) 185-189.

© 2015 The Authors. Published by ESG ([www.electrochemsci.org](http://www.electrochemsci.org)). This article is an open access article distributed under the terms and conditions of the Creative Commons Attribution license (<http://creativecommons.org/licenses/by/4.0/>).